

Missing spectral weight in a paramagnetic heavy-fermion system

Jingwen Li,¹ Debankit Priyadarshi,¹ Chia-Jung Yang,¹ Ulli Pohl,² Oliver Stockert,³
Hilbert von Löhneysen,⁴ Shovon Pal,^{5,*} Manfred Fiebig,^{1,†} and Johann Kroha^{2,6,‡}

¹*Department of Materials, ETH Zurich, 8093 Zurich, Switzerland*

²*Physikalisches Institut and Bethe Center for Theoretical Physics, University of Bonn, 53115 Bonn, Germany*

³*Max Planck Institute for Chemical Physics of Solids, 01187 Dresden, Germany*

⁴*Institut für Quantenmaterialien und -technologien and Physikalisches Institut,
Karlsruhe Institute of Technology, 76021 Karlsruhe, Germany*

⁵*School of Physical Sciences, National Institute of Science Education and Research, HBNI, Jatni, 752 050 Odisha, India*

⁶*School of Physics and Astronomy, University of St. Andrews,
North Haugh, St. Andrews, KY16 9SS, United Kingdom*

(Dated: August 15, 2024)

The competition between the Kondo spin-screening effect and the Ruderman-Kittel-Kasuya-Yosida (RKKY) interaction in heavy-fermion systems drives the quantum phase transition between the magnetically ordered and the heavy-Fermi-liquid ground states. Despite intensive investigations of heavy quasiparticles on the Kondo-screened side of the quantum phase transition and of their breakdown at the quantum critical point, studies on the magnetically ordering side are scarce. Using terahertz time-domain spectroscopy, we report a suppression of the Kondo quasiparticle weight in $\text{CeCu}_{6-x}\text{Au}_x$ samples on the antiferromagnetic side of the quantum phase transition at temperatures as much as two orders of magnitude above the Néel temperature T_N . The suppression results from a quantum frustration effect induced by the temperature-independent RKKY interaction. Hence, our results emphasize that besides critical fluctuations, the RKKY interaction may play an important role in the quantum-critical scenario.

Keywords: Strongly-correlated materials, heavy-fermions, THz spectroscopy, quantum phase transition

I. INTRODUCTION

Heavy-fermion materials are prototypes of strongly interacting systems that contain a matrix of localized magnetic moments in $4f$ orbitals, immersed in a sea of mobile conduction electrons¹⁻³. The hybridization of localized $4f$ electrons with conduction electrons generates (i) the Kondo spin-exchange coupling J between local and itinerant moments⁴, and (ii) in the second order of J , a long-range correlation between distant local moments, the Ruderman-Kittel-Kasuya-Yosida (RKKY) interaction⁵⁻⁷. The local moments are screened by the conduction spins due to the Kondo effect^{3,8}. In contrast to charge screening, spin screening is a quantum effect which leads to a many-body entangled, singlet ground state below the binding energy. The latter is given roughly by³ the lattice Kondo temperature $T_K^* \approx D e^{-1/(2N_0J)}$, where D is the half bandwidth, and N_0 is the conduction density of states at the Fermi level E_F . The excitations of this state are complex quantum superpositions of localized and itinerant states, the heavy, fermionic quasiparticles which form a narrow band near E_F ^{3,9}. On the other hand, the RKKY interaction, which scales as $T_{\text{RKKY}} \approx N_0 J^2$, tends to order the magnetic moments and, thus, counteracts the Kondo spin screening. Therefore, Doniach¹⁰ put forward a schematic heavy-fermion phase diagram which consists of a spin-screened, heavy-Fermi-liquid (HFL) phase realized at low temperatures $T \lesssim T_K^*$ when the Kondo scale dominates over the RKKY energy, $T_K^* > T_{\text{RKKY}}$, and a magnetically ordered phase for $T_{\text{RKKY}} > T_K^*$. In the heavy-fermion compound $\text{CeCu}_{6-x}\text{Au}_x$, for example, substituting Cu by Au reduces the spin-exchange coupling J and, thus, leads to the phase

diagram shown in Fig. 1(a); see below for more details. The HFL and the antiferromagnetic (AFM) phases are separated by a quantum critical point (QCP) at $x = x_c = 0.1$ where T_K^* and T_{RKKY} balance each other.

The behavior of the heavy, fermionic quasiparticles near the quantum phase transition (QPT) have been a subject of intense discussion, since their breakdown can give way to the formation of novel quantum states of matter beyond the Fermi-liquid paradigm. Quantum-critical scenarios driven by different types of critical fluctuations have been proposed for the quantum phase transition across the quantum-critical point (QCP) in heavy-fermion compounds. These include local quantum criticality¹¹⁻¹³, Fermi surface fluctuations¹⁴, or long-range antiferromagnetic fluctuations¹⁵⁻¹⁷. In the spin-density-wave scenario, the HFL is formed below T_K^* and undergoes a spin-density-wave instability at a critical spin coupling or Fermi-surface nesting. In this case, the QPT is driven by the critical fluctuations of the bosonic order parameter (staggered magnetization) only, and the fermionic quasiparticles remain intact across the transition¹⁸⁻²⁰. In the local quantum-critical scenario¹¹⁻¹³, order-parameter fluctuations couple to the local Kondo spins and destroy the heavy fermionic quasiparticles near the QPT. Furthermore, it was shown generally²¹ and supported by numerical renormalization-group calculations for two-impurity systems with conduction-electron-induced RKKY coupling^{22,23} that complete spin screening ceases to exist beyond a critical RKKY coupling strength. This is caused by a quantum frustration effect, which subsequently gives way to the magnetic ordering of the incompletely screened spins.

Terahertz time-domain spectroscopy (THz-TDS) pro-

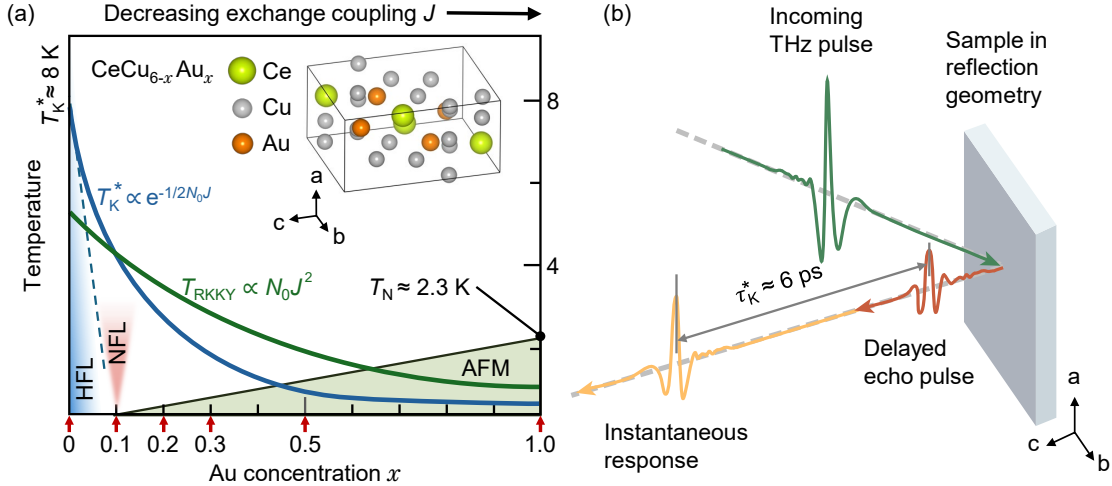


Figure 1. (a) Quantum phase transition in $\text{CeCu}_{6-x}\text{Au}_x$ from the HFL phase to the antiferromagnetically ordered phase, parameterized by the non-thermal control parameter x . While the RKKY interaction scales as $T_{\text{RKKY}} \propto N_0 J(x)^2$, the Kondo energy scales as $T_{\text{K}}^* \approx D e^{-1/(2N_0 J)}$, where J decreases with the increase of x . The QCP occurs at the critical substitution $x_c = 0.1$ where $T_{\text{RKKY}} \approx T_{\text{K}}^*$. The inset shows the orthorhombic crystal structure of the $\text{CeCu}_{6-x}\text{Au}_x$ system. (b) Schematic of the experimental geometry showing the incident and the reflected THz pulses on the sample. Upon THz excitation, a fraction of the correlated Kondo states gets destroyed. It then takes the Kondo coherence time τ_{K}^* for the reconstruction of the heavy-quasiparticle state, accompanied by the emission of a characteristic echo pulse in the THz range at a delay of $\approx \tau_{\text{K}}^*$.

vides a unique, background-free means to investigate the spectral weight of heavy quasiparticles^{24–27}. Specifically, the emission of a characteristic, time-delayed echo pulse after an irradiated THz pulse separates the correlation-induced Kondo spectral weight from other contributions. In the present work, we use this THz-TDS approach to systematically scrutinize the behavior of the quasiparticle weight in the prototypical heavy-fermion compound $\text{CeCu}_{6-x}\text{Au}_x$ ²⁸. We cover the complete range of Au concentrations, $0.0 \leq x \leq 1.0$, in particular, covering the region of supercritical Au concentration ($x > x_c$) and above the AFM ordering temperature T_{N} .

On the HFL side of the QPT, where the Kondo scale is set by $T_{\text{K}}^* \approx 8\text{K}$ ^{2,24}, the heavy-quasiparticle weight starts to build up already at temperatures as high as $\sim 130\text{K}$ due to the logarithmic onset of Kondo correlations²⁴. Therefore, one might expect the same behavior on the AFM side far above T_{N} , where AFM critical fluctuations are absent. Surprisingly, however, our experiments show that in this strongly substituted regime, the Kondo weight is systematically suppressed, even far above T_{N} . As we will discuss, this is a clear indication for the importance of the temperature-independent RKKY interaction for the QPT in this system.

II. SAMPLES AND EXPERIMENTAL METHOD

Single crystals of $\text{CeCu}_{6-x}\text{Au}_x$ were grown by the Czochralski method^{28–31} and are freshly polished using colloidal silica before the THz-TDS measurements^{24,25}. The surface roughness during sample preparation is within the

sub-micrometer range, significantly below the wavelength of THz radiation. The concentrations of Au used in this work are $x = 0.0, 0.1, 0.2, 0.3, 0.5$, and 1.0 , marked by the red arrows in Fig. 1(a). The samples are mounted in a Janis SVT-400 helium reservoir cryostat with a controlled temperature environment ranging from 300K down to 2K .

Substitution of Cu by the larger Au atoms expands the host lattice while maintaining the orthorhombic structure, see inset of Fig. 1(a). This reduces the Ce $4f$ conduction-electron hybridization and, hence, the exchange coupling J . Considering the parametric dependence of T_{K}^* and T_{RKKY} on J and following Doniach’s argument¹⁰, below the critical Au concentration of $x < x_c = 0.1$, a spin-screened HFL phase is stabilized below the Kondo-scale temperature T_{K}^* ^{2,32}. For $x > x_c$, an incommensurate AFM phase is realized³³. For $x = 1.0$, the Néel temperature is $T_{\text{N}} \approx 2.3\text{K}$ with a linear decrease of T_{N} as a function of x as the QCP at $x_c = 0.1$ is approached^{2,34}.

In the experiment, single-cycle, linearly polarized THz pulses are generated via optical rectification in a 0.5-mm -thick (110)-cut ZnTe generation crystal, using up to 90% of an amplified Ti:sapphire laser output (wavelength of 800nm , pulse duration of 120fs , repetition rate of 1kHz , pulse energy of 1.5mJ). The THz light pulses are then guided onto the sample using off-axis parabolic mirrors. As the samples are metallic, we collect the signal in a reflection geometry, as shown in Fig. 1(b). We measure both the time-dependent amplitude and phase of the reflected THz light by free-space electro-optic sampling, using the residual 10% of the laser output as the sampling light. The THz and the sampling beams are collinearly focused onto a 0.5-mm -thick, (110)-cut ZnTe detection crystal. The THz-

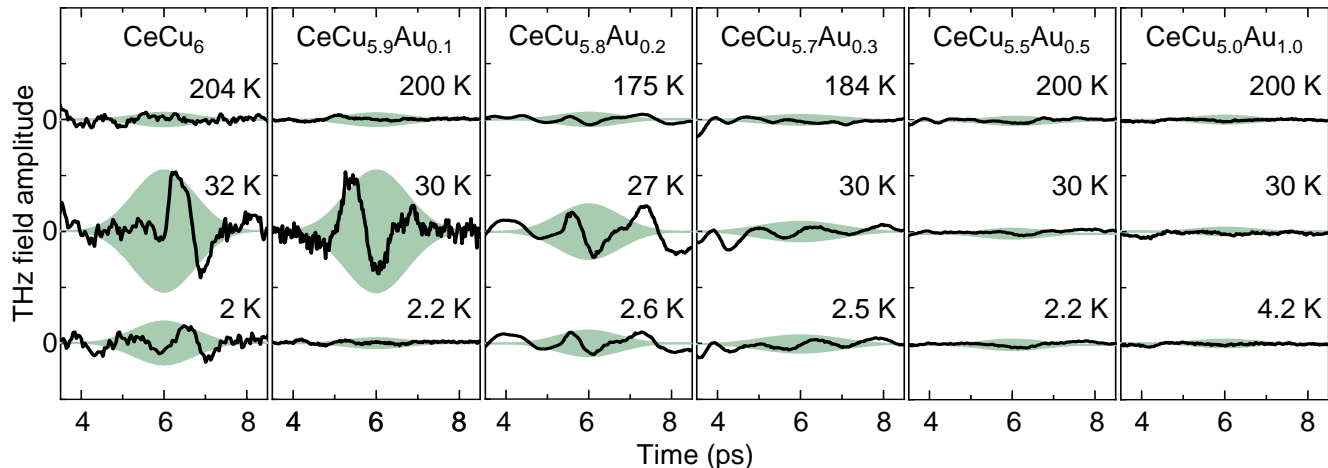


Figure 2. Normalized THz time traces in reflection from the $\text{CeCu}_{6-x}\text{Au}_x$ samples in three different temperature ranges. The green-shaded area depicts the envelope of the time-delayed THz reflex, containing the coherent contributions from the heavy quasiparticles. The envelope is obtained from the solution of the nonlinear rate equation as discussed in Ref. [24]. Note that a temperature-independent background signal is present at all temperatures. It has been determined close to room temperature where the Kondo weight is undetectably small, and subtracted from the signal at all temperatures²⁴.

light-induced ellipticity of the sampling beam is then measured using a quarter-wave plate, a Wollaston prism, and a balanced photodiode. In order to increase the accessible delay time between the THz pump and the optical probe pulses, Fabry-Pérot resonances from the faces of the detection crystal are suppressed by an additional 2-mm-thick, THz-inactive (100)-cut ZnTe single crystal that is optically bonded to the back of the detection crystal. All measurements are performed in an inert N_2 atmosphere.

III. RESULTS AND DISCUSSION

When our heavy-fermion material interacts with the THz radiation, a fraction of the correlated Kondo states gets destroyed^{24–27}. In other words, the excitation leads to an electronic interband transition from the heavy-fermion band into the light part of the conduction band³⁵, breaking the Kondo singlet and thereby deleting the associated spectral weight of the heavy band. The reconstruction of the heavy-quasiparticle state happens on the scale of the Kondo coherence time $\tau_K^* = 2\pi\hbar/k_B T_K^*$, when the relaxing electrons emit a characteristic, echo-like pulse at a delay time τ_K^* . The echo response is background-free and bears distinct information on the Kondo correlation dynamics^{24,27}. It is a fingerprint of the electronic coherence that is intrinsic to the heavy bands³⁶ and is separated in the time-domain from the instantaneous response which arises from intra-band excitations, see the schematic illustration in Fig. 1(b). The echo-pulse intensity and delay time are measures of the quasiparticle weight and their intrinsic coherence time τ_K^* , respectively. A quantitative comparison between the $\text{CeCu}_{6-x}\text{Au}_x$ samples with different Au concentrations is then obtained by normalizing the THz signals with respect to the area of the samples.

To navigate through the phase diagram, we investigate

the $\text{CeCu}_{6-x}\text{Au}_x$ sample with $x = 0$, exhibiting an HFL ground state, the quantum-critical sample with $x = 0.1$, and samples with $x = 0.2, 0.3, 0.5$, and 1.0 , featuring an AFM ground state^{2,32,33}. We deliberately show our measured data for $x = 0.2, 0.3, 0.5$ along with published data at $x = 0.0, 0.1, 1.0$ ²⁴ because only the direct comparison of the two sets reveals the stark difference in the response on the low- and high-substitution sides of the QCP with a previously unrecognized behavior on the latter side.

Fig. 2 shows the traces of the THz transients reflected from our samples for three representative temperature ranges each, normalized to the total reflected power and the sample area²⁴. We use a fixed time window^{24,25} for the investigation of the delayed response across all the $\text{CeCu}_{6-x}\text{Au}_x$ samples. By integrating the echo pulse within this time window, we calculate the heavy-quasiparticle spectral weight²⁴.

Figure 3(a) depicts the temperature-dependent quasiparticle spectral weight for our $\text{CeCu}_{6-x}\text{Au}_x$ series. For the heavy-fermion (CeCu_6) and the quantum-critical ($\text{CeCu}_{5.9}\text{Au}_{0.1}$) compounds, the spectral weight builds up from around 130 K and increases logarithmically down to 30 K as the manifestation of the Kondo effect. Upon further reducing the temperature, the spectral weight of the quantum-critical sample drops continuously and reaches an undetectably small value for $T < 5$ K, indicating quasiparticle disintegration near the QCP²⁴. In CeCu_6 , the spectral weight reaches the same maximum as for the quantum-critical sample, yet it settles to a finite value toward lowest temperatures, roughly 40% beneath than its maximum. This finite, but decreased spectral weight reflects the HFL ground state in proximity to the QCP.

Beyond the QCP, that is, for the $\text{CeCu}_{6-x}\text{Au}_x$ samples with $x > 0.1$, the temperature dependence of the data recorded for the present work exhibits a strikingly different and quite surprising behavior in comparison to the

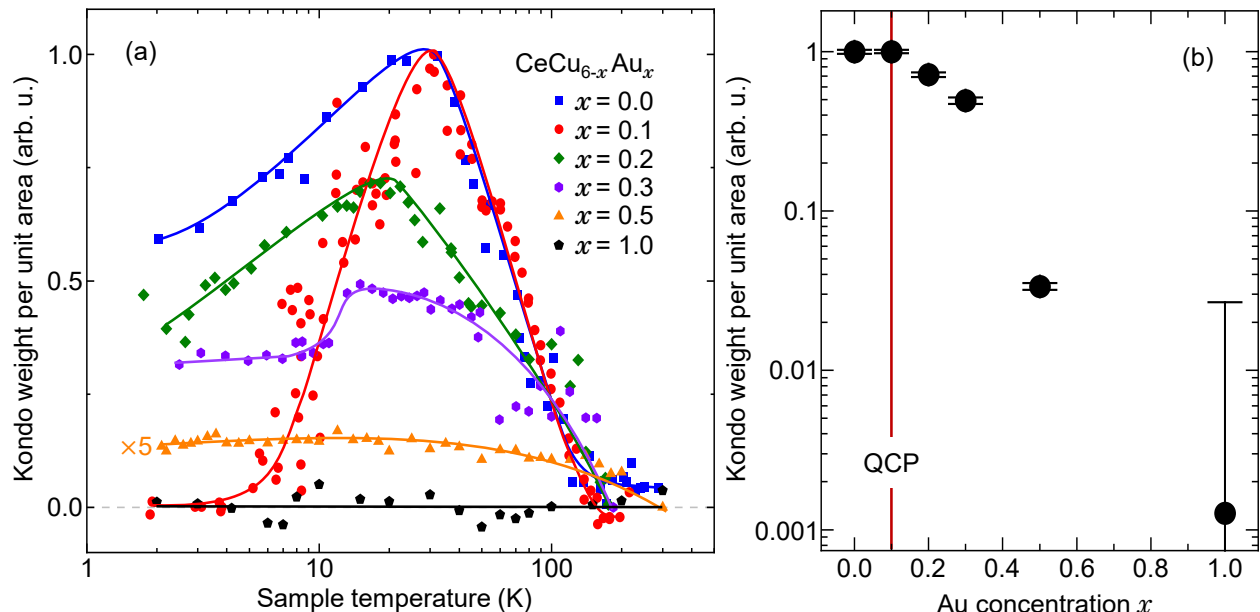


Figure 3. (a) Temperature dependence of the Kondo weight per unit area of our $\text{CeCu}_{6-x}\text{Au}_x$ samples. Published data²⁴ ($x = 0.0, 0.1, 1.0$) are shown along with our new data ($x = 0.2, 0.3, 0.5$) for better accentuation of the different responses on the low- and high-substitution sides of the QCP. The weight is derived from the integrated intensity of the reflected THz echo pulse, see Fig. 2. The solid lines are guides to the eye. (b) The Kondo spectral weight per unit area of $\text{CeCu}_{6-x}\text{Au}_x$ as a function of Au concentration x at the temperature associated with the fitted maximum of the Kondo weight in (a) (except for $x = 1$ where we average the entire data set).

data at $x < 0.1$. We observe a pronounced decrease in the maximum Kondo weight with increasing x . While in $\text{CeCu}_{5.8}\text{Au}_{0.2}$ as well as in $\text{CeCu}_{5.7}\text{Au}_{0.3}$ the Kondo spectral weight shows a similar onset near 130K, its build-up weakens as x increases, and it reaches a maximum lower than for the HFL sample ($x = 0$), before it settles to a reduced value at the lowest temperatures; see also Ref. [37]. At $x = 0.5$, the Kondo weight is still non-zero, yet barely detectable, and it has vanished entirely at $x = 1.0$. This x dependence of the Kondo weight is shown in Fig. 3(b) for the respective fitted maximum of the temperature-dependent Kondo-weight data in Fig. 3(a) (except for $x = 1$ where we average the entire data set). While the decrease in maximum weight with x is moderate for $x = 0.2$ and $x = 0.3$, a steep decline occurs beyond $x = 0.3$. We suspect that this reflects the x -dependent exponential decrease of the Kondo energy with respect to the RKKY interaction, T_K^*/T_{RKKY} , as sketched in Fig. 1, but further samples and analysis would be required to support this assumption.

Figure 4 shows the phase diagram of $\text{CeCu}_{6-x}\text{Au}_x$ where the Kondo spectral weight, represented through by the color code, has been interpolated from the samples with $x = 0, 0.1, 0.2, 0.3, 0.5$, and 1.0 available for this study. The figure clearly demonstrates that the Kondo destruction at $x \gtrsim 0.4$ occurs in the high-temperature region of the phase diagram where critical AFM order-parameter fluctuations are absent. The destruction must, therefore, be caused by the RKKY interaction alone, which is active at all temperatures. Such RKKY-induced breakdown has been predicted in Refs. [21] and [22] and is due to a quan-

tum frustration effect between Kondo spin screening and inter-impurity RKKY interaction. Specifically, When coupled to the spin of a distant Kondo ion, a local impurity spin cannot freely fluctuate to form a singlet with the surrounding conduction electrons. Similar Kondo destruction has been found in scanning-tunneling-spectroscopy experiments on CoCu_nCo clusters ($n \geq 3$) on $\text{Cu}(111)$ ³⁸ and on a continuously tunable two-impurity Kondo system of Co adatoms on the tip and on $\text{Au}(111)$ ³⁹. We observe this effect here in a bulk Kondo-lattice system. We would also like to stress that the Kondo breakdown region around $x = 0.4$ is well separated from the quantum-critical region around $x_c = 0.1$. It indicates that the effect of RKKY-related quantum frustration and the effect of critical fluctuations emerge independently. Hence, the QPT is most probably induced by cooperation of RKKY-induced frustration of spin screening and critical fluctuations of the AFM order parameter¹¹⁻¹³.

IV. CONCLUSION

In conclusion, we have investigated the behavior of the heavy-quasiparticle weight across the quantum phase transition induced in the $\text{CeCu}_{6-x}\text{Au}_x$ system by tuning the Au concentration. While a logarithmic build-up of spectral weight is observed when the Kondo effect dominates over the RKKY interaction ($x \leq 0.1$), in the $\text{CeCu}_{6-x}\text{Au}_x$ compounds with $x > 0.1$ the heavy quasiparticle spectral weight is significantly suppressed and essentially vanishes

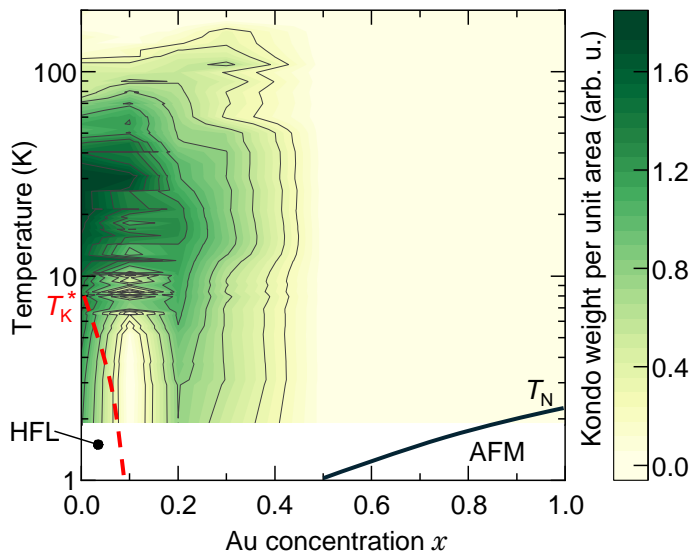


Figure 4. Phase diagram of $\text{CeCu}_{6-x}\text{Au}_x$ obtained by tuning the Au concentration. The color code represents the heavy-quasiparticle spectral weight. Near the QCP, the quasiparticle weight decreases as a result of critical fluctuations. In contrast, the missing heavy quasiparticle spectral weight beyond $x \approx 0.4$ is caused by the RKKY-induced frustration of Kondo-singlet formation.

for $x > 0.5$. Most unusually, this behavior occurs at tem-

peratures much higher than the magnetic ordering temperature, that is, in the paramagnetic phase. Our results point to the importance of the frustration effect of the RKKY interaction on the formation of the heavy-fermion singlet formation. The separation of the RKKY-induced breakdown from the quantum phase transition at $x_c = 0.1$ in the phase diagram suggests that the former emerges independent of the latter, implying that the QPT is the result of the cooperation of both RKKY-induced frustration of the spin screening and critical fluctuations of the AFM order parameter.

V. ACKNOWLEDGEMENT

J.L., D.P., C.-J.Y., and M.F. acknowledge the financial support from the Swiss National Science Foundation through Projects No. 200021_178825 and No. 200021_219807. S.P. acknowledges the support from DAE through the project Basic Research in Physical and Multi-disciplinary Sciences via RIN4001. S.P. also acknowledges the startup support from DAE through NISER and SERB through SERB-SRG via Project No. SRG/2022/000290. J.K. acknowledges the support of the Deutsche Forschungsgemeinschaft via TRR 185 (277625399) OSCAR, project C4, and the Cluster of Excellence ML4Q (90534769).

S.P., M.F., and J.K. contributed equally to this work.

* shovon.pal@niser.ac.in

† manfred.fiebig@mat.ethz.ch

‡ kroha@physik.uni-bonn.de

- ¹ P. Coleman, Heavy Fermions: Electrons at the Edge of Magnetism, Handbook of Magnetism and Advanced Magnetic Materials Vol. 1 (Wiley, New York, 2007), pp. 95-148.
- ² H. von Löhneysen, A. Rosch, M. Vojta, and P. Wölfle, Fermi-liquid instabilities at magnetic quantum phase transitions, *Rev. Mod. Phys.* **79**, 1015 (2007).
- ³ A. C. Hewson, The Kondo problem to heavy fermions (Cambridge University Press, Cambridge, England, 1993).
- ⁴ P. W. Anderson, Localized magnetic states in metals, *Phys. Rev.* **124**, 41 (1961).
- ⁵ M. A. Ruderman, and C. Kittel, Indirect exchange coupling of nuclear magnetic moments by conduction electrons, *Phys. Rev.* **96**, 99 (1954).
- ⁶ T. Kasuya, A theory of metallic ferro- and antiferromagnetism on Zener's model, *Prog. Theor. Phys.* **16**, 45 (1956).
- ⁷ K. Yosida, Magnetic properties of Cu-Mn alloys, *Phys. Rev.* **106**, 893 (1957).
- ⁸ J. Kondo, Resistance minimum in dilute magnetic alloys, *Prog. Theor. Phys.* **32**, 37 (1964).
- ⁹ P. Li, H. Ye, Y. Hu, Y. Fang, Z. Xiao, Z. Wu, Z. Shan, R. P. Singh, G. Balakrishnan, D. Shen, Y.-F. Yang, C. Cao, N. C. Plumb, M. Smidman, M. Shi, J. Kroha, H. Yuan, F. Steglich, and Y. Liu, Photoemission signature of the competition between magnetic order and Kondo effect in CeCoGe_3 , *Phys. Rev. B* **107**, L201104 (2023).
- ¹⁰ S. Doniach, Kondo lattice and weak antiferromagnetism,

Physica B+C **91**, 231 (1977).

- ¹¹ Q. Si, S. Rabello, K. Ingersent, and J. L. Smith, Locally critical quantum phase transitions in strongly correlated metals, *Nature (London)* **413**, 804 (2001).
- ¹² P. Coleman, C. Pépin, Q. Si, and R. Ramazashvili, How do Fermi liquids get heavy and die? *J. Phys. Condens. Matter* **13**, R723 (2001).
- ¹³ Q. Si, S. Rabello, K. Ingersent, and J. L. Smith, Local fluctuations in quantum critical metals, *Phys. Rev. B* **68**, 115103 (2003).
- ¹⁴ T. Senthil, M. Vojta, and S. Sachdev, Weak magnetism and non-Fermi liquids near heavy-fermion critical points, *Phys. Rev. B* **69**, 035111 (2004).
- ¹⁵ P. Wölfle, and E. Abrahams, Quasiparticles beyond the Fermi liquid and heavy fermion criticality, *Phys. Rev. B* **84**, 041101(R) (2011).
- ¹⁶ E. Abrahams, J. Schmalian, and P. Wölfle, Strong-coupling theory of heavy-fermion criticality, *Phys. Rev. B* **90**, 045105 (2014).
- ¹⁷ P. Wölfle, and E. Abrahams, Vertex functions at finite momentum: Application to antiferromagnetic quantum criticality, *Phys. Rev. B* **93**, 075128 (2016).
- ¹⁸ J. A. Hertz, Quantum critical phenomena, *Phys. Rev. B* **14**, 1165 (1976).
- ¹⁹ A. Millis, Effect of a nonzero temperature on quantum critical points in itinerant fermion systems, *Phys. Rev. B* **48**, 7183 (1993).
- ²⁰ T. Moriya, Spin fluctuations in itinerant electron magnetism (Springer, Berlin, 1985).

- ²¹ A. Nejadi, K. Ballmann, and J. Kroha, Kondo destruction in RKKY-coupled Kondo lattice and multi-impurity systems, *Phys. Rev. Lett.* **118**, 117204 (2017).
- ²² K. P. Wójcik and J. Kroha, Quantum spin liquid in an RKKY-coupled two-impurity Kondo system, *Phys. Rev. B* **107**, L12111 (2023).
- ²³ K. P. Wójcik and J. Kroha, Asymmetry effects on the phases of RKKY-coupled two-impurity Kondo systems, *Phys. Rev. B* **107**, 125146 (2023).
- ²⁴ C. Wetli, S. Pal, J. Kroha, K. Kliemt, C. Krellner, O. Stockert, H. von Löhneysen, and M. Fiebig, Time-resolved collapse and revival of the Kondo state near a quantum phase transition, *Nat. Phys.* **14**, 1103 (2018).
- ²⁵ S. Pal, C. Wetli, F. Zamani, O. Stockert, H. von Löhneysen, M. Fiebig, and J. Kroha, Fermi volume evolution and crystal-field excitations in heavy-fermion compounds probed by time-domain terahertz spectroscopy, *Phys. Rev. Lett.* **122**, 096401 (2019).
- ²⁶ C.-J. Yang, J. Li, M. Fiebig, and S. Pal, Terahertz control of many-body dynamics in quantum materials, *Nat. Rev. Mater.* **8**, 518 (2023).
- ²⁷ C.-J. Yang, K. Kliemt, C. Krellner, J. Kroha, M. Fiebig, and S. Pal, Critical slowing down of fermions near a magnetic quantum phase transition, *Nat. Phys.* **19**, 1605 (2023).
- ²⁸ H. von Löhneysen, T. Pietrus, G. Portisch, H. G. Schlager, A. Schröder, M. Sieck, and T. Trappmann, Non-Fermi-liquid behavior in a heavy-fermion alloy at a magnetic instability, *Phys. Rev. Lett.* **72**, 3262 (1994).
- ²⁹ H. von Löhneysen, Fermi-liquid instability at magnetic-nonmagnetic quantum phase transitions, *J. Magn. Magn. Mater.* **200**, 532 (1999).
- ³⁰ H. G. Schlager, A. Schröder, M. Welsch, and H. von Löhneysen, Magnetic ordering in $\text{CeCu}_{6-x}\text{Au}_x$ single crystals: Thermodynamic and transport properties, *J. Low Temp. Phys.* **90**, 181 (1993).
- ³¹ N. Neubert, T. Pietrus, O. Stockert, H. von Löhneysen, A. Rosch, and P. Wölfle, Electrical resistivity of the non-Fermi-liquid alloy $\text{CeCu}_{5.9}\text{Au}_{0.1}$, *Phys. B: Condens. Matter* **230-232**, 587 (1997).
- ³² A. Amato, D. Jaccard, J. Flouquet, F. Lapiere, J. L. Tholence, R. A. Fisher, S. E. Lacy, J. A. Olsen, and N. E. Phillips, Thermodynamic and transport properties of CeCu_6 , *J. Low Temp. Phys.* **68**, 371 (1987).
- ³³ H. von Löhneysen, A. Neubert, T. Pietrus, A. Schröder, O. Stockert, U. Tutsch, M. Loewenhaupt, A. Rosch, and P. Wölfle, Magnetic order and transport in the heavy-fermion system $\text{CeCu}_{6-x}\text{Au}_x$, *Eur. Phys. J. B* **5**, 447 (1998).
- ³⁴ T. Pietrus, B. Bogenberger, S. Mock, M. Sieck, and H. von Löhneysen, Pressure dependence of the Néel temperature in antiferromagnetic $\text{CeCu}_{6-x}\text{Au}_x$ for $0.3 \leq x \leq 1.3$, *Physica B* **206-207**, 317 (1995).
- ³⁵ C.-J. Yang, S. Pal, F. Zamani, K. Kliemt, C. Krellner, O. Stockert, H. von Löhneysen, J. Kroha, and M. Fiebig, Terahertz conductivity of heavy-fermion systems from time-resolved spectroscopy, *Phys. Rev. Research* **2**, 033296 (2020).
- ³⁶ C.-J. Yang, M. Woerner, O. Stockert, H. von Löhneysen, J. Kroha, M. Fiebig, and S. Pal, Kondo coherence versus superradiance in a terahertz radiation-driven heavy-fermion systems, *Phys. Rev. B* **109**, 235103 (2024).
- ³⁷ M. Klein, A. Nuber, F. Reinert, J. Kroha, O. Stockert, and H. v. Löhneysen, Signature of quantum criticality in photoemission spectroscopy, *Phys. Rev. Lett.* **101**, 266404 (2008).
- ³⁸ N. Néel, R. Berndt, J. Kröger, T. O. Wehling, A. I. Lichtenstein, and M. I. Katsnelson, Two-site Kondo effect in atomic chains, *Phys. Rev. Lett.* **107**, 106804 (2011).
- ³⁹ J. Bork, Y.-H. Zhang, L. Diekhöner, L. Borda, P. Simon, J. Kroha, P. Wahl, and K. Kern, A tunable two-impurity Kondo system in an atomic point contact, *Nat. Phys.* **7**, 901 (2011).